

Modeling of Plasma Current Decay during the Disruption

H. Ohwaki^{1,2}, M. Sugihara³, Y. Kawano¹, V.E. Lukash⁴, R.R. Khayrutdinov⁵,
V. Zhogolev⁴, T. Ozeki¹, A. Hatayama²

¹ Japan Atomic Energy Research Institute, Naka-shi, Ibaraki-ken, Japan 311-0193

² Keio University, Hiyoshi, Yokohama, Japan 223-8522

³ ITER International Team, Naka JWS, Naka-shi, Ibaraki-ken, Japan 311-0193

⁴ RRC Kurchatov Institute for Atomic Energy, Moscow, Russian Federation

⁵ TRINITI, Troitsk, Russian Federation

1. Introduction

Electromagnetic (EM) forces by the disruption on the in-vessel components and vacuum vessel sometimes become significantly large in tokamaks, especially in ITER with large plasma current I_p . Thus, an accurate estimation of the EM forces is of primary importance in ITER design. These EM forces are induced by the rapid plasma current reduction during the current quench, and it is essential to evaluate the decay time of the plasma current for the EM forces. Although the minimum current decay time expected in ITER is examined using the disruption database of existing tokamaks [1], this guideline is not fully based on the physical mechanism of disruptions. Therefore, we have to develop a reliable numerical model for the estimation of the current decay time.

The simplest way to evaluate the decay time is to use the L_{eff}/R_p time. Here, L_{eff} is the effective plasma inductance and R_p is the plasma resistance. However, changes of the plasma MHD equilibrium during the current decay influence L_{eff} and R_p , so that a more rigorous model is needed. In this paper, a detailed model is developed, which solves rate equations for densities of fuel and impurities, and determines the electron temperature and plasma resistivity by power balance. In addition, this model is incorporated with the DINA simulation code [2], which calculates an evolution of the plasma MHD equilibrium and circuit equations consistently to obtain the plasma current. Simulations are compared with fast disruptions in JT-60U. Essential parameters to govern the current decay are demonstrated.

2. Numerical model

2.1. Densities of hydrogen, impurities and electrons

The densities of hydrogen and impurities of the k -th charge state n_s^k are solved with the following equation.

$$\frac{dn_s^k}{dt} = \langle \sigma v \rangle_{\text{ion}}^{k-1} n_s^{k-1} n_e - \left(\langle \sigma v \rangle_{\text{ion}}^k + \langle \sigma v \rangle_{\text{rec}}^k \right) n_s^k n_e + \langle \sigma v \rangle_{\text{rec}}^{k+1} n_s^{k+1} n_e - \frac{n_s^k}{\tau_s^*}, \quad (1)$$

where

$$n_e = n_H^1 + \sum_{k=1}^N k n_z^k, \quad (2)$$

n_e , n_H^1 and n_z^k are the densities of electrons, protons and impurities of the k -th charge state, respectively. Ionization rate coefficients $\langle \sigma v \rangle_{\text{ion}}^k$ and recombination rate coefficients $\langle \sigma v \rangle_{\text{rec}}^k$ for hydrogen and impurities of the k -th charge state are tabulated as a function of the electron temperature T_e in the ADAS code [3]. Diffusion and recycling of particles are taken into account by introducing the effective residence time τ_s^* .

2.2. Power balance

When the thermal quench occurs, sputtered or evaporated impurities from the plasma facing components penetrate into the plasma. During the current quench phase, the impurity content is usually very high, so that the impurity radiation is much larger than the ordinary transport loss and auxiliary heating. This radiation loss power density $P_{\text{rad}} = n_e \sum_{k=0}^N n_z^k L_z^k$ is then balanced with the joule heating power density $P_{\text{joule}} = \eta j^2$ converted from the magnetic energy of the plasma current at a certain temperature. Here, L_z^k is the emissivity of the k -th charge state impurities, which is tabulated as a function of T_e in the ADAS. The current density j is assumed to be uniform in the plasma cross-section. We use the Spitzer resistivity for η [4]. From this power balance equation, T_e and η are determined.

$$P_{\text{joule}}(T_e) = P_{\text{rad}}(T_e). \quad (3)$$

To obtain an evolution of the plasma current and equilibrium, the DINA code is simultaneously solved with Eqs. (1) – (3). In the circuit equation of the plasma current in the DINA, precise evaluations of T_e and η are of primary importance.

3. Comparison with experiments

In this model, the density including all charge state particles of hydrogen n_H and impurities n_z just after the thermal quench, and the effective residence time of hydrogen τ_H^* and impurities τ_z^* are given as adjustable parameters to reproduce experiments. By changing these parameters, a set of parameters, $n_H = 10^{20} \text{ m}^{-3}$, $n_z = 7 \times 10^{19} \text{ m}^{-3}$ at $t = 7038 \text{ ms}$, $\tau_H^* = 25 \text{ ms}$ and $\tau_z^* = 2 \text{ ms}$, which can reproduce the experimental I_p waveform for a shot #31708 in JT-60U, is obtained (Fig. 1). In this set, only carbon is considered as impurities. Fig. 2 shows the evolution of the plasma boundary. The cross-sectional area S decreases with the I_p decay

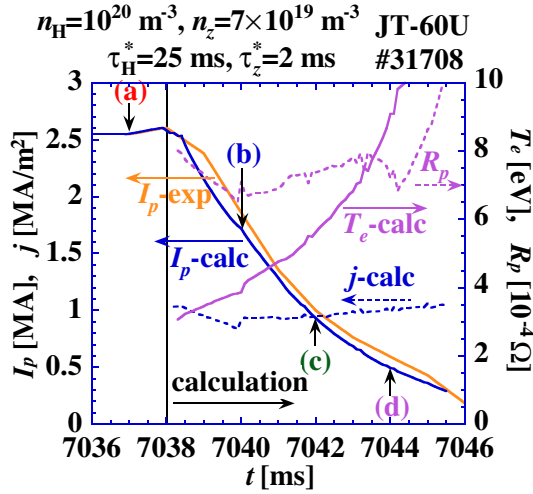


Fig. 1: Time evolutions of I_p , j , T_e and R_p which can reproduce the experiment (#31708).

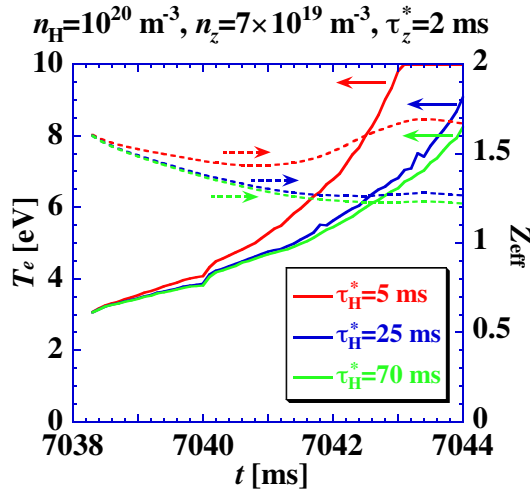


Fig. 3: T_e and Z_{eff} for various τ_{H}^* .

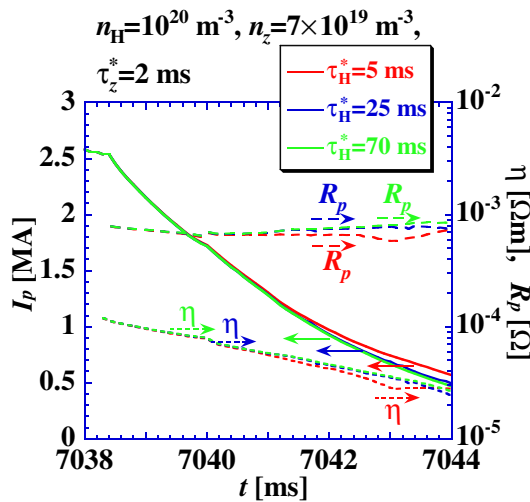


Fig. 4: I_p , η and R_p for various τ_{H}^* .

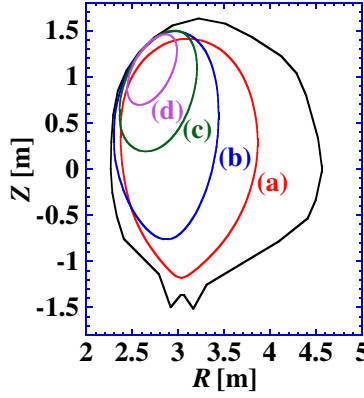


Fig. 2: Time evolutions of the plasma boundary (LCFS) for the case of Fig. 1 at four time points.

and j is almost constant for this case. During this I_p decay the impurity density decreases with the time scale τ_z^* , and P_{rad} is reduced. As a result of the power balance, T_e increases and P_{joule} is reduced. The effective plasma inductance changes a little, and thus, the I_p decay rate is dominated by the plasma resistance, $R_p \sim Z_{\text{eff}} / (T_e^{3/2} S)$. Here, Z_{eff} is the effective charge. In the present case, although the plasma resistivity $\eta \sim Z_{\text{eff}} / T_e^{3/2}$ decreases, the change of R_p is not large and the decay rate is almost constant, i.e., exponential-like decay of I_p .

To investigate dependencies of the characteristics of the I_p decay on those parameters, we change parameters from the condition of Fig. 1. It is found that variations of n_{H} and τ_{H}^* influence the I_p decay only weakly. It is because η and R_p do not change so much by compensation between Z_{eff} and T_e . For example, if τ_{H}^* is larger than the case of Fig. 1, the electron density becomes larger. This makes both Z_{eff} and T_e smaller (Fig. 3). Then R_p and I_p decay rate changes very mildly (Fig. 4). Consequently, the I_p decay depends on n_{H} and τ_{H}^* only weakly.

To the contrary, variations of n_z and τ_z^* significantly influence the I_p decay. The reason is

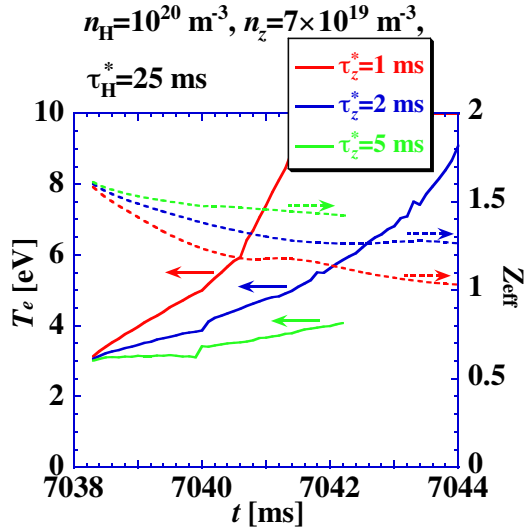


Fig. 5: T_e and Z_{eff} for various τ_z^* .

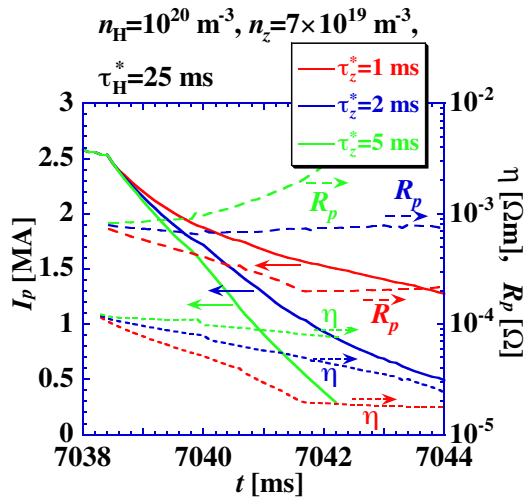


Fig. 6: I_p , η and R_p for various τ_z^* .

that changes of Z_{eff} and T_e caused by these variations enhance the changes of η and R_p . For example, if τ_z^* is larger, the impurity density decreases slowly, which makes Z_{eff} larger and T_e lower (Fig. 5). As a result, larger R_p makes the I_p decay faster (Fig. 6). In this way, the I_p decay strongly depends on n_z and τ_z^* .

4. Conclusions

We have developed a numerical model to simulate the plasma current decay after the thermal quench. This model can reproduce the experimental results of the I_p evolution in JT-60U with reasonable parameters. Characteristics of the I_p evolution during the current quench are clarified by changing n_H , n_z , τ_H^* and τ_z^* . First, the amount of impurities and its residence time in the plasma are dominant parameters to reproduce the experimental I_p decay rate because they significantly influence the power balance, i.e. the electron temperature. Secondly, the electron temperature tends to rise with the decrease of I_p due to the decrease of

impurities with almost constant current density. Plasma shrinkage plays an important role for this phase. These factors are necessary to reproduce the experimental I_p decay waveform.

Acknowledgements

The authors are grateful to Dr. T. Takizuka for his valuable discussions and supports. We are also grateful to Drs. T. Nakano and K. Shimizu for their arrangement in using the ADAS code.

References

- [1] M. Sugihara, et al., Proc. 20th IAEA FEC, Vilamoura (2004), IT/P3-29.
- [2] R.R. Khayrutdinov, V.E. Lukash, J. Comput. Phys. **109**, 193 (1993).
- [3] H.P. Summers, JET-IR06 (1994), <http://adas.phys.strath.ac.uk/>.
- [4] NRL plasma formulary, 2000, p. 34.